



# An evaluation of Global Satellite Mapping of Precipitation (GSMaP) datasets over Iran

Mohammad Darand<sup>1,2</sup> · Zeinab Siavashi<sup>1</sup>

Received: 27 November 2020 / Accepted: 24 February 2021 / Published online: 11 March 2021  
© The Author(s), under exclusive licence to Springer-Verlag GmbH Austria, part of Springer Nature 2021

## Abstract

This study aimed to quantitatively evaluate three GSMAp products including near-real-time (GSMAp-NRT), microwave-infrared reanalyzed (GSMAp-MVK), and gauge-adjusted (GSMAp-Gauge) data with a spatial resolution of  $0.1^\circ \times 0.1^\circ$  versus gauge-observed data (observation) at daily and monthly time scales over Iran. Different statistical metrics including correlation coefficient (R), percent bias (PBias), root mean square error (RMSE), probability of detection (POD), false alarm ratio (FAR), and critical success index (CSI) were used to evaluate the capability of the GSMAp products. The results indicated that all three products were generally capable of capturing the spatial pattern of precipitation. However, they all overestimated precipitation in general, and there was a considerable difference between the two satellite-only products GSMAp-MVK and GSMAp-NRT and the gauge-corrected product GSMAp-Gauge. GSMAp-Gauge performed better than the other products at both daily and monthly time scales. The evaluations demonstrated that all the GSMAp products provided better estimations of precipitation over Western than Eastern Iran. The strongest agreement between the products and the observed data was observed for the rainy months, while performance was poor for the dry months. The findings could help GSMAp product developers to better understand the characteristics of the involved errors.

## 1 Introduction

As a key determining factor in the understanding of the hydrological cycle, the Earth's energy balance, and various socioeconomic activities, precipitation often exhibits high spatiotemporal variability (Su et al. 2014; Ning et al. 2016; Kidd and Huffman 2011). Ground-based rain gauge observation is the main physically direct and the most commonly used method for measurement of precipitation, and is still deemed as the most accurate tool for observation of precipitation (Petersen et al. 2005). However, the great spatial heterogeneity of rain gauges is a considerable challenge, particularly in areas with complex topography like Iran. Recently, satellite-based precipitation estimates have turned

into an attractive alternative resource, providing complete data in data-sparse or ungauged regions with their extensive spatial coverage and fine space and time resolutions, which can overcome the challenges involved in sparse or uneven distributions of rain gauge stations (Tian et al. 2010; Chen et al. 2016; Cifelli et al. 2011; Sugiarto et al. 2017; Peng et al. 2014; Vergara et al. 2014; Sun et al. 2016).

Among the several satellite-based precipitation products, microwave radiometers have been demonstrated as measuring precipitation fairly accurately from low Earth orbit satellites (Ushio et al. 2009; Dinku et al. 2010). However, they involve uncertainties and errors that can be affected by precipitation estimation algorithms, cloud reflectance, thermal radiance, and infrequent satellite overpasses (Khodadoust Siuki et al. 2017), which may vary from region to region or from season to season (Darand et al. 2017; Hosseini-Moghari and Tang 2020).

The Global Satellite Mapping of Precipitation (GSMAp) is a precipitation product with high spatial resolution started in 2002, supported by the Japan Science and Technology Agency (JST) and Japan Aerospace Exploration Agency (JAXA) (Kubota et al. 2007). The aim of GSMAp is to generate a high-precision, high-resolution precipitation map using satellite data by blending infrared radiometer (IR) and

---

Responsible Editor: Sang-Woo Kim.

---

✉ Mohammad Darand  
m.darand@uok.ac.ir

<sup>1</sup> Department of Climatology, Faculty of Natural Resources, University of Kurdistan, Sanandaj, Iran

<sup>2</sup> Department of Zrebar Lake Environmental Research, Kurdistan Studies Institute, University of Kurdistan, Sanandaj, Iran

passive microwave (PMW) data (Kummerow et al. 1998; Okamoto et al. 2005).

Several studies have been conducted to evaluate GSMAp products versus rain gauge observation over different regions in the world. For example, Ushio et al. (2009) verified the performance of GSMAp-MVK with rain gauge data over Japan. The results indicated that GSMAp-MVK matched well with the rain gauge observation, but underestimated large precipitation amounts. Prakash et al. (2016) evaluated TMPA-3B42 and GSMAp precipitation products over the Indian monsoon region using a gridded gauge-based rainfall dataset and found that TMPA-3B42V7 was closer to gauge-based observation. They reported a systematic underestimation of precipitation by the GSMAp-MVK and GSMAp-NRT datasets. Zhao et al. (2018) quantitatively evaluated three GSMAp products including near-real-time (GSMAp-NRT), microwave-infrared reanalyzed (GSMAp-MVK), and gauge-adjusted (GSMAp-Gauge) data against gauge-observed data (CPAP) over China. Although GSMAp-Gauge underestimates precipitation, it presented significantly improved metrics over mainland China and the eight subregions as compared to GSMAp-NRT and GSMAp-MVK, and performed better than them in terms of the statistical metrics. According to Trinh-Tuan et al. (2019), GSMAp agreed relatively well among several satellite precipitation datasets with surface rainfall observation over Central Vietnam at multiple spatial and temporal scales.

Wang and Yong (2020) analyzed the accuracy of GSMAp and Integrated Multi-satellite Retrievals for Global Precipitation Measurement (IMERG) products versus rain gauge observation at the near-global scale from the aspects of latitude, season, and elevation. They reported that both IMERG and GSMAp products performed reasonably well in summer but poorly in winter, and tended to overestimate precipitation in high-latitude areas of the Northern Hemisphere and also in areas with low rainfall intensity.

To our knowledge, there is no published work on the evaluation of GSMAp products over Iran. This study, therefore, evaluated three GSMAp products versus gauge observation over Iran. The GSMAp products included the standard microwave-IR combined (GSMAp-MVK), gauge-corrected (GSMAp-Gauge), and near-real-time (GSMAp-NRT) products.

## 2 Study area, data, and methods

### 2.1 Study area

Lying within the  $25^{\circ}$ – $40^{\circ}$  range of latitudes and the  $44^{\circ}$ – $64^{\circ}$  range of longitudes, Iran is one of the largest countries in the Middle East with an area of 1,648,000 km $^2$ . The terrain shows a complex topography with high mountains in

the western and northern regions and deserts in the central region. Due to the arid and semi-arid climate, the area-averaged annual precipitation is approximately 250 mm. Precipitation exhibits high spatial variations from over 1800 mm in the southwestern Caspian coastal region in the North to less than 50 mm in the central desert region.

## 2.2 Data

### 2.2.1 GSMAp precipitation data

GSMAp is a global precipitation product combining PMW and IR data to estimate high temporal (hourly) and spatial ( $0.1^{\circ}$ ) resolution precipitation values from a latitudinal belt of  $60^{\circ}$  N– $60^{\circ}$  S. In the current study, three GSMAp products, including the near-real-time product GSMAp-NRT, standard research product GSMAp-MVK, and gauge-calibrated product GSMAp-Gauge, were evaluated for the period from 1 March 2014 to 31 December 2018 over Iran, with the assumption of consistent the data production periods. Both GSMAp-NRT and GSMAp-MVK use a technique known as the Kalman filter model to compute precipitation and combine PMW and IR data, but they differ in terms of the input satellite datasets (Prakash et al. 2016). GSMAp-NRT uses only forward propagation, while both forward and backward propagation are applied in GSMAp-MVK (Ushio et al. 2009). GSMAp-Gauge is a gauge-calibrated version of GSMAp-MVK, adjusted by the Climate Prediction Center (CPC) global gauge datasets (Zhao et al. 2017).

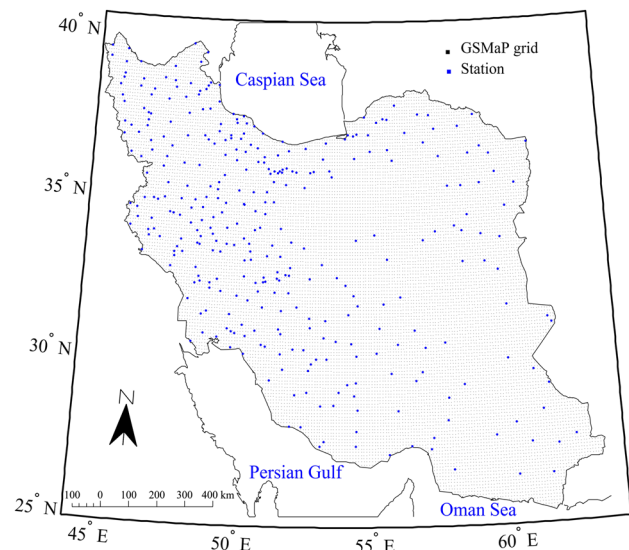


**Fig. 1** Study area along with the GSMAp grids and rain gauge stations

## 2.2.2 Gauge precipitation data

To evaluate the GSMAp products, we used the three-hourly point observational precipitation data obtained from 344 rain gauge stations (Fig. 1) operated by the Iranian Meteorological Organization (IRIMO). The gauge network is fairly dense in Western and Northern Iran but uneven and sparse in the central and eastern regions. In Iran, rain observations are made daily covering a 24 h accumulation period from 9.30 a.m. of 1 day until 9.30 a.m. of the next. For this reason, the daily-accumulated precipitation values for the GSMAp products were computed for each grid on a particular day through the summation of the 1 h values for the same time span as that mentioned above before the evaluations were processed. The daily precipitation measurements were also aggregated to a monthly scale for monthly statistical comparisons.

## 2.3 Methods

For the quantitative evaluation of the GSMAp products, the following widely-applied statistical metrics were used: correlation coefficient ( $R$ ), root mean square error (RMSE), percent bias (PBias), probability of detection (POD), false alarm ratio (FAR), and critical success index (CSI). The equations for these indices are described below:

$$R = \frac{\sum_{i=1}^N (P_i - \bar{P})(O_i - \bar{O})}{\sqrt{\sum_{i=1}^N (P_i - \bar{P})^2} \sqrt{\sum_{i=1}^N (O_i - \bar{O})^2}}, \quad (1)$$

$$PBias = \frac{\sum_{i=1}^n (p_i - o_i)}{\sum_{i=1}^n o_i} \times 100, \quad (2)$$

$$RMSE = \sqrt{\frac{\sum_{i=1}^n (p_i - o_i)^2}{n}}, \quad (3)$$

$$POD = \frac{RR}{RR + RN}, \quad (4)$$

$$FAR = \frac{NR}{RR + NR}, \quad (5)$$

$$CSI = \frac{RR}{RR + RN + NR}, \quad (6)$$

where  $O$  represents the gauge-observed data,  $P$  indicates the GSMAp data, and  $n$  is the number of samples. In Eqs. (4) to (6), RR shows the number of times that observed rain is correctly detected, NN denotes the number of times that

rain is neither observed nor detected, RN signifies the number of times that observed rain is not detected, and NR is the number of times that rain is detected but not observed. POD and FAR range from 0 to 1, with 1 and 0 being perfect scores, respectively. CSI also ranges from 0 to 1, with 1 indicating a perfect detection. Taylor diagrams were also used to visualize and quantify the overall performance of the GSMAp products.

## 3 Results and discussions

### 3.1 Spatial distribution of precipitation

Figure 2 shows the spatial distribution of total annual precipitation for observation and the GSMAp products over Iran during the study period from 2014 to 2018. From the observation (Fig. 1), it can be noted that precipitation exhibited high spatial heterogeneity, with high precipitation observed over the southwestern coast of Caspian Sea and the Zagros Mountain ranges in the West and low precipitation observed over the central deserts. Clearly, the GSMAp products performed reasonably well in capturing of the spatial distribution of precipitation, and there was a general declining trend from the West to the East. In general, the spatial patterns of annual total precipitation appeared to be similar in GSMAp-MVK and GSMAp-NRT, which differed in magnitude, however. Both GSMAp-MVK and GSMAp-NRT overestimated precipitation over the western and northwestern regions and some parts of the northern region while exhibiting less precipitation along the southwestern coast of the Caspian Sea than in the gauge-based observation data, considerably improved in GSMAp-Gauge. This may be explained by the forward or backward propagation process used in the GSMAp-MVK and GSMAp-NRT algorithms, leaving out some short-lived convection precipitation events that occur in warm months, which results in more events with no precipitation (Deng et al. 2018). Generally, the overestimation made in GSMAp-MVK was slightly larger than that in GSMAp-NRT. Among the three GSMAp products, GSMAp-Gauge clearly exhibited a spatial distribution of precipitation most similar to observation and performed best in terms of total annual precipitation.

### 3.2 Spatial statistical analysis

Pattern correlation ( $R$ ) is a measure of association between two different time series data in the representation of precipitation features (Sperber et al. 2013). Figure 3 shows the spatial distributions of the correlation coefficient ( $R$ ) in the three GSMAp products versus observation at daily and monthly scales. It is clear from the figure that all the products exhibited high correlations ( $> 0.7$ ) in the western region, where

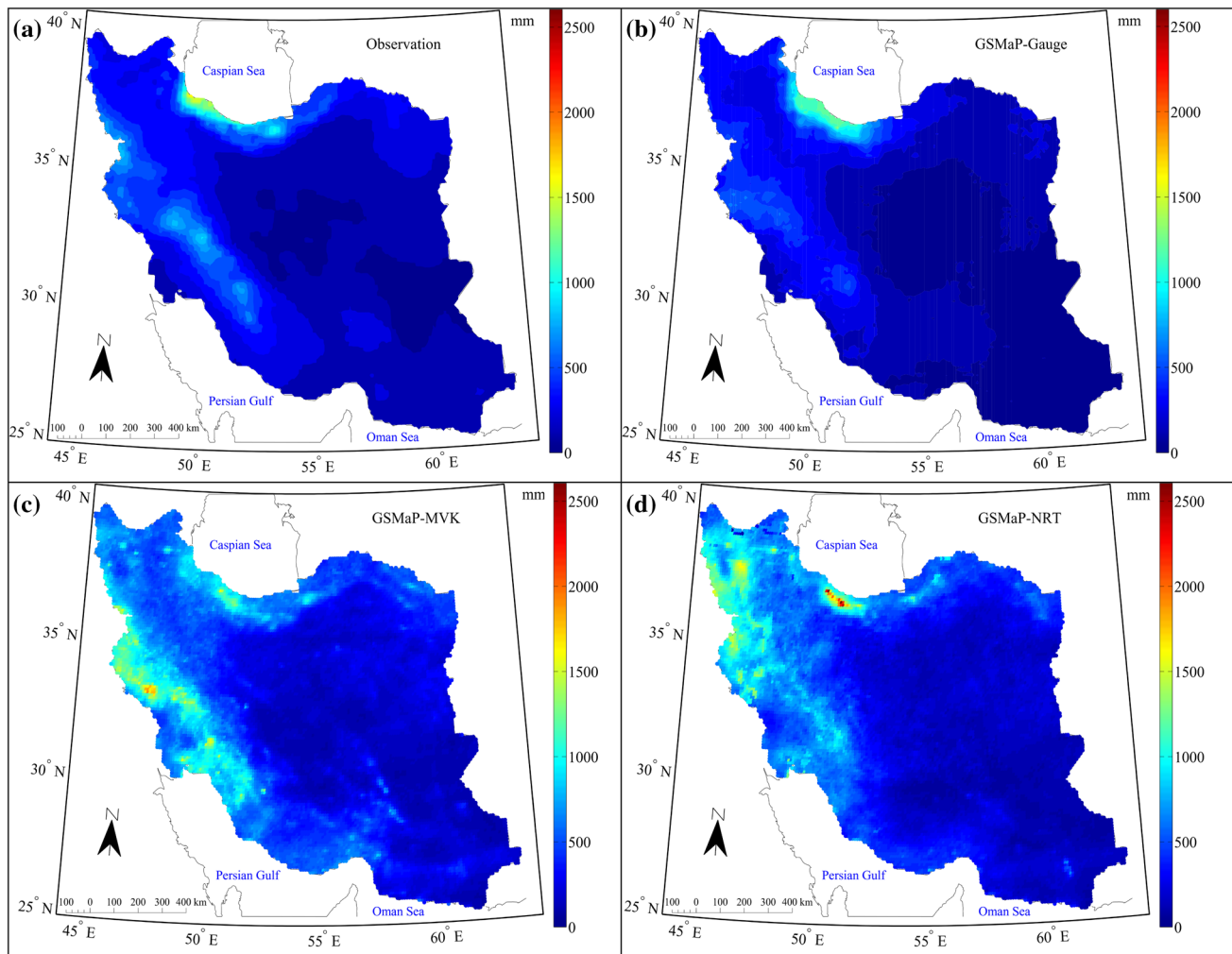
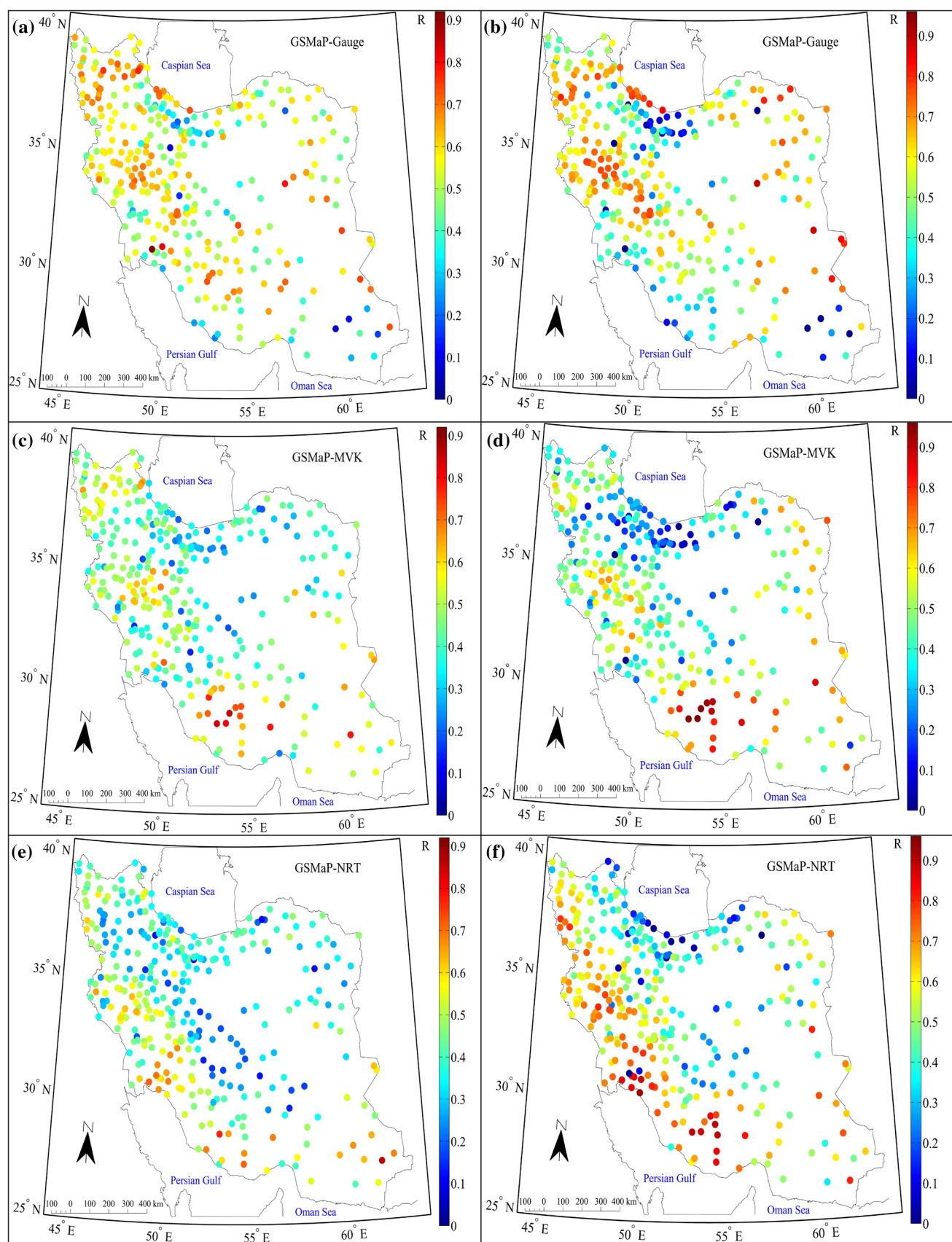


**Fig. 2** Spatial distributions of total annual precipitation from **a** gauge-based observation, **b** GSMAp-Gauge, **c** GSMAp-MVK, and **d** GSMAp-NRT

precipitation is high. Low correlations ( $<0.2$ ) were found in the central region and the Alborz Mountain ranges in the North. The lower correlation coefficients in Northern Iran could be attributed to the complex topography and high spatial and temporal heterogeneity of precipitation, in line with the previous findings (e.g., AghaKouchak et al. 2012; Chen et al. 2013; Beck et al. 2017; Gebregiorgis et al. 2017). The low correlation in the central region might be due to the low-density gauge network, decreasing the accuracy of gauge-based geostatistical analysis (Xie et al. 2007). GSMAp-NRT exhibited much better performance at a monthly scale than at a daily scale. A comparison of the GSMAp-Gauge and GSMAp-MVK correlation coefficient patterns demonstrated that the former outperformed the latter, indicating that the optimal scheme introduced in the GSMAp-Gauge algorithm provided well-adjusted GSMAp-MVK estimations as compared to the CPC data, in line with the observations made in Mega et al. (2018) and Zhao et al. (2018) for the equivalent data over China. Figure 4 compares the area-averaged time

**Fig. 3** Spatial distributions of R between observation and GSMAp-Gauge (a, b), GSMAp-MVK (c, d), and GSMAp-NRT (e, f) at daily (left panel) and monthly (right panel) time scales

series of daily and monthly precipitation for the observation data and the GSMAp products. The three products exhibited similar day-to-day and month-to-month precipitation variability, but there were some discrepancies. The PBias values indicated that all the three GSMAp products exhibited positive relative bias, and involved overestimation, which was more evident for GSMAp-MVK. In line with the findings of Zhao et al. (2018) over China, GSMAp-NRT performed better than GSMAp-MVK over Iran. GSMAp-MVK overestimated daily and monthly precipitation by about 74% and 104%, respectively. Although GSMAp-Gauge exhibited a lower R than GSMAp-NRT, it had the lowest PBias and RMSE, which suggested that GSMAp-Gauge was better than the other GSMAp products in those terms at both daily and



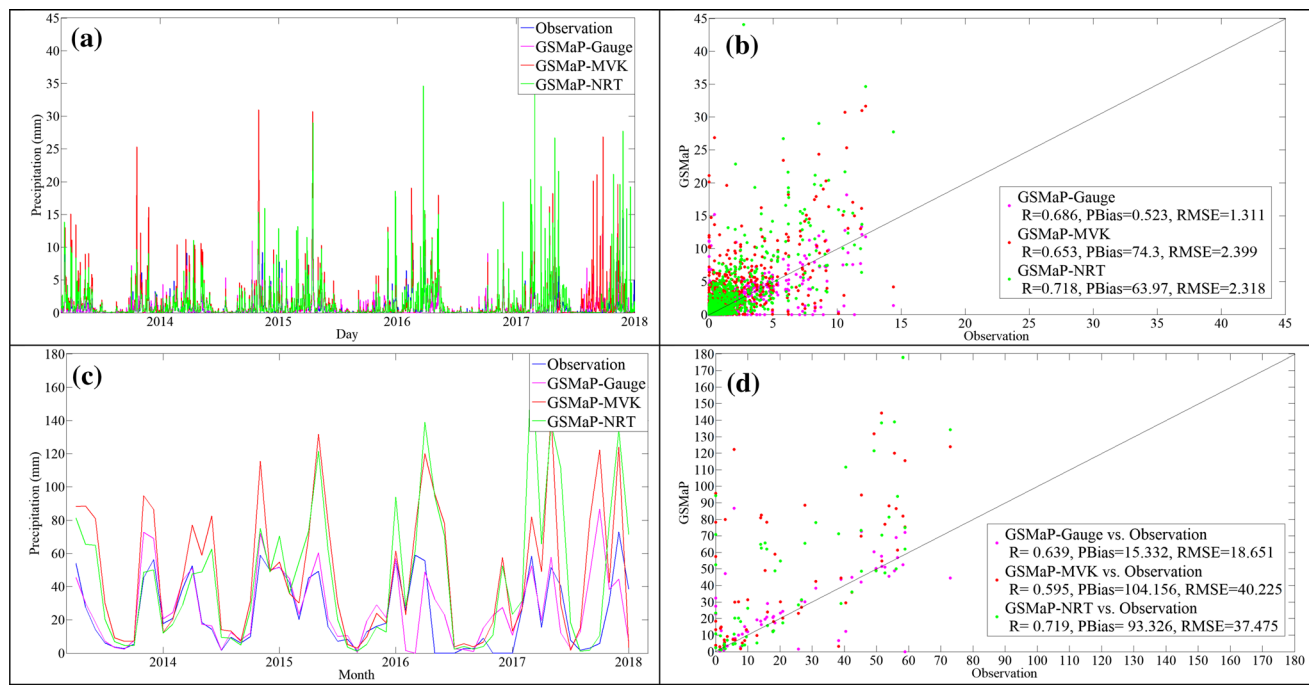


**Fig. 4** Area-averaged time series of daily (a) and monthly (c) precipitation for the observation data and the GSMAp products. Scatter plots between the observation data and the GSMAp products at daily (b) and monthly (d) time scales

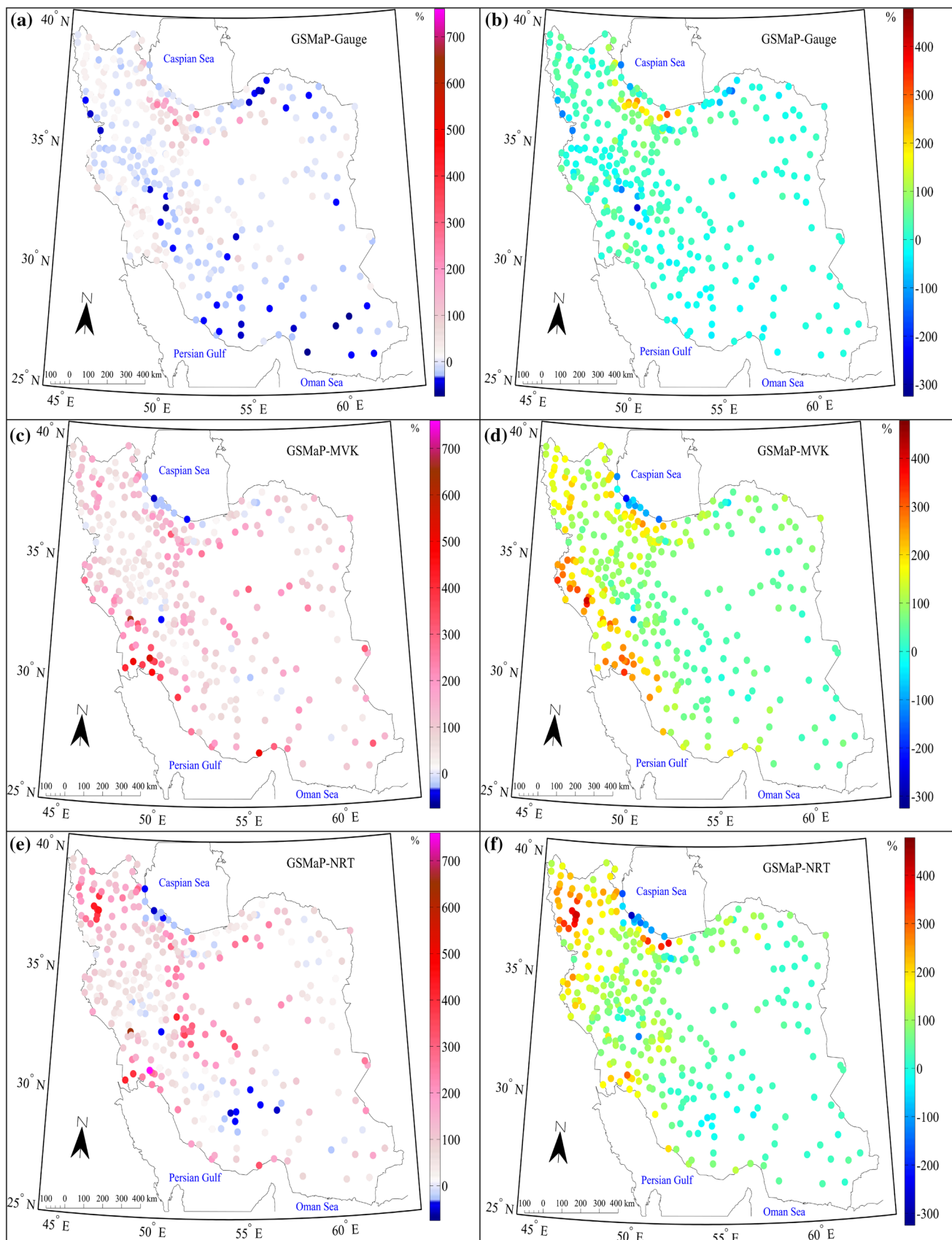
monthly time scales. This was consistent with the results shown in Fig. 2.

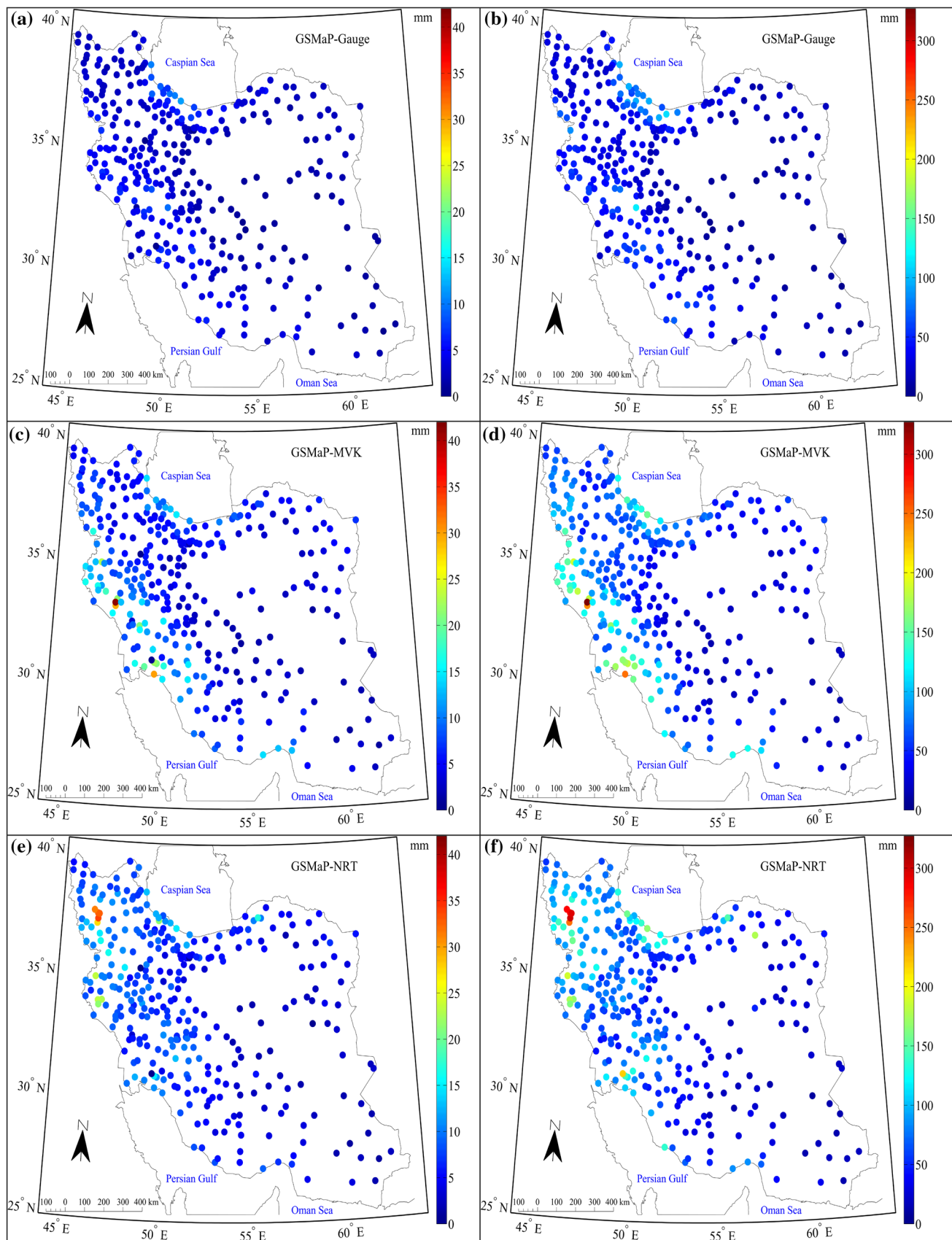
The spatial distributions of PBias for the GSMAp products could provide valuable information, particularly for analysis of bias propagation in local to regional hydrological and climatological applications. Figure 5 shows PBias for the GSMAp products against the observation data. Negative values indicate GSMAp product underestimation bias, while positive values indicate overestimation bias (Gupta et al. 1999). It is clear from Fig. 5 that the GSMAp products overestimated precipitation over the entire territory except for some areas in Southern Iran and the southwestern coast of the Caspian Sea in the North. GSMAp-Gauge effectively reduced the systematic errors of GSMAp-MVK with bias correction using the CPC gauge analysis precipitation dataset. Although GSMAp-Gauge was calibrated with the CPC gauge precipitation data, it underestimated precipitation by 20% on average, with a higher magnitude of underestimation over Southern Iran and the Zagros Mountain range. This could be explained by the poor quality of the adjusted data source due to the sparse data and the satellite-gauge blending algorithm of GSMAp-Gauge. The other two products (GSMAp-MVK and GSMAp-NRT) largely overestimated precipitation in the southwestern and northwestern regions of Iran, with PBias values over 550% and 450% at daily and monthly scales, respectively.

Figure 6 shows the spatial distributions of RMSE in the GSMAp products versus observation, which were the same at daily and monthly time scales. For PBias, the highest values for GSMAp-MVK and GSMAp-NRT were observed in Southwestern and Northwestern Iran and the southwestern coastal region of the Caspian Sea in the North. GSMAp-Gauge exhibited much lower RMSE values than the other GSMAp products (< 3 mm/day and < 30 mm/month) over most parts of Iran. This suggests that the gauge adjustments were significantly different in the correction of the PBias and RMSE values.

Figures 7 and 8 present the spatial distributions of POD, FAR, and CSI for the GSMAp products versus observation. In terms of POD, GSMAp-MVK and GSMAp-NRT exhibited similar spatial distributions. The gauge-adjusted GSMAp-Gauge product performed better than GSMAp-MVK and GSMAp-NRT in most of Iran except the southeastern region. Spatially, GSMAp-MVK and GSMAp-NRT provided the best performance over Southern and Southwestern Iran, while they exhibited the worst performance over the central desert region, as evidenced by the smallest POD (less than 0.5), greatest FAR (more than 0.7), and smallest CSI (less than 0.3). Furthermore, GSMAp-MVK had considerably poorer

**Fig. 5** Spatial distributions of PBias in GSMAp-Gauge (a, b), GSMAp-MVK (c, d), and GSMAp-NRT (e, f) versus observation at daily (left panel) and monthly (right panel) time scales





**Fig. 6** Spatial distributions of RMSE for GSMAp-Gauge (**a**, **b**), GSMAp-MVK (**c**, **d**), and GSMAp-NRT (**e**, **f**) versus observation at daily (left panel) and monthly (right panel) time scales

performance than GSMAp-NRT in terms of FAR and CSI. The poor performance of the satellite products in the detection of precipitation in the desert region could be due in part to the possible evaporation of raindrops before reaching the ground in arid environments (Behrangi et al. 2014). It should be noted that the largest POD and CSI values for GSMAp-Gauge occurred in the Zagros Mountain ranges in the West and the southwestern coastal region of the Caspian Sea in the North. The results were generally better for the gauge-adjusted product GSMAp-Gauge than the others, which could be attributed to the gauge-based corrections in that product.

To determine which GSMAp product most precisely estimated precipitation over Iran, Taylor diagrams (Taylor 2001) were plotted to visualize a statistical summary of how well each product matched the reference gauge-observation data in terms of three statistical metrics, namely correlation coefficient, normalized centered root mean square difference (RMSD), and normalized standard deviation. The location of each color circle appearing on a Taylor diagram quantified how closely the GSMAp product matched the reference observation data. The closer a GSMAp product to the reference observation data, the better the estimate.

As shown in Fig. 9a, GSMAp-Gauge exhibited lower standard deviation and RMSD values than GSMAp-MVK and GSMAp-NRT. Overall, GSMAp-Gauge was closer to the observation values than GSMAp-MVK and GSMAp-NRT at a daily time scale, and presented the best overall performance, followed by GSMAp-NRT and GSMAp-MVK.

For further investigation of the performance of the GSMAp products, Taylor diagrams were plotted for each GSMAp product at a monthly scale. The analysis indicated that all the three GSMAp products exhibited good performance during March, April, January, and December when most of the precipitation occurs in Iranian climate. The relative differences were much greater in August, September, and June, when precipitation amounts are generally small, and there are dry conditions in the Iranian climate due to the dominance of high subtropical pressure at middle tropospheric levels (Darand and Mirzaei 2020). This finding was in line with previous studies (e.g. Fu et al. (2011) over China, Hur et al. (2016) over Singapore, Fatkhuroyan et al. (2018) over Indonesia, and Salles et al. (2019) over Brazil's

central plateau region). The overall performance of the three GSMAp products in the retrieval of monthly precipitation was similar to that in the daily precipitation estimates, indicating higher performance for GSMAp-Gauge than for the other products, which can be accounted for by the improvement made in the gauge-corrected GSMAp-MVK.

## 4 Conclusion

The main findings of the study are summarized below.

1. The GSMAp products properly captured the spatial distribution pattern of precipitation over Iran, particularly over the western region.
2. Except for some areas in Southern Iran and the southwestern coast of the Caspian Sea in the North, all the three GSMAp products overestimated precipitation over Iran.
3. Based on the statistical metrics and spatial precipitation patterns, GSMAp-Gauge performed better than the other two products. However, there were still some monitoring errors in the gauge-adjusted precipitation satellite product GSMAp-Gauge, which could be explained by the poor quality of the adjusted data source due to the sparse data and satellite-gauge blending algorithm.
4. Even though R, PBias, and RMSE were comparable in GSMAp-MVK and GSMAp-NRT, GSMAp-NRT performed better than GSMAp-MVK over Iran.
5. GSMAp-Gauge exhibited a much higher POD/CSI and a much lower FAR than the other two GSMAp products. It should be noted that the largest POD and CSI values for GSMAp-Gauge were obtained in the Zagros Mountain ranges in the West and the southwestern coastal region of the Caspian Sea in the North. GSMAp-MVK and GSMAp-NRT exhibited similar spatial distributions in terms of POD, while GSMAp-MVK provided considerably poorer performance than GSMAp-NRT in terms of FAR and CSI. GSMAp-MVK and GSMAp-NRT exhibited the best performance over Southern and Southwestern Iran but the worst performance over the central desert region, as evidenced by the smallest POD (less than 0.5), greatest FAR (more than 0.7), and smallest CSI (less than 0.3).
6. All the three GSMAp products exhibited good performance during the rainy months and poor performance during the dry months.

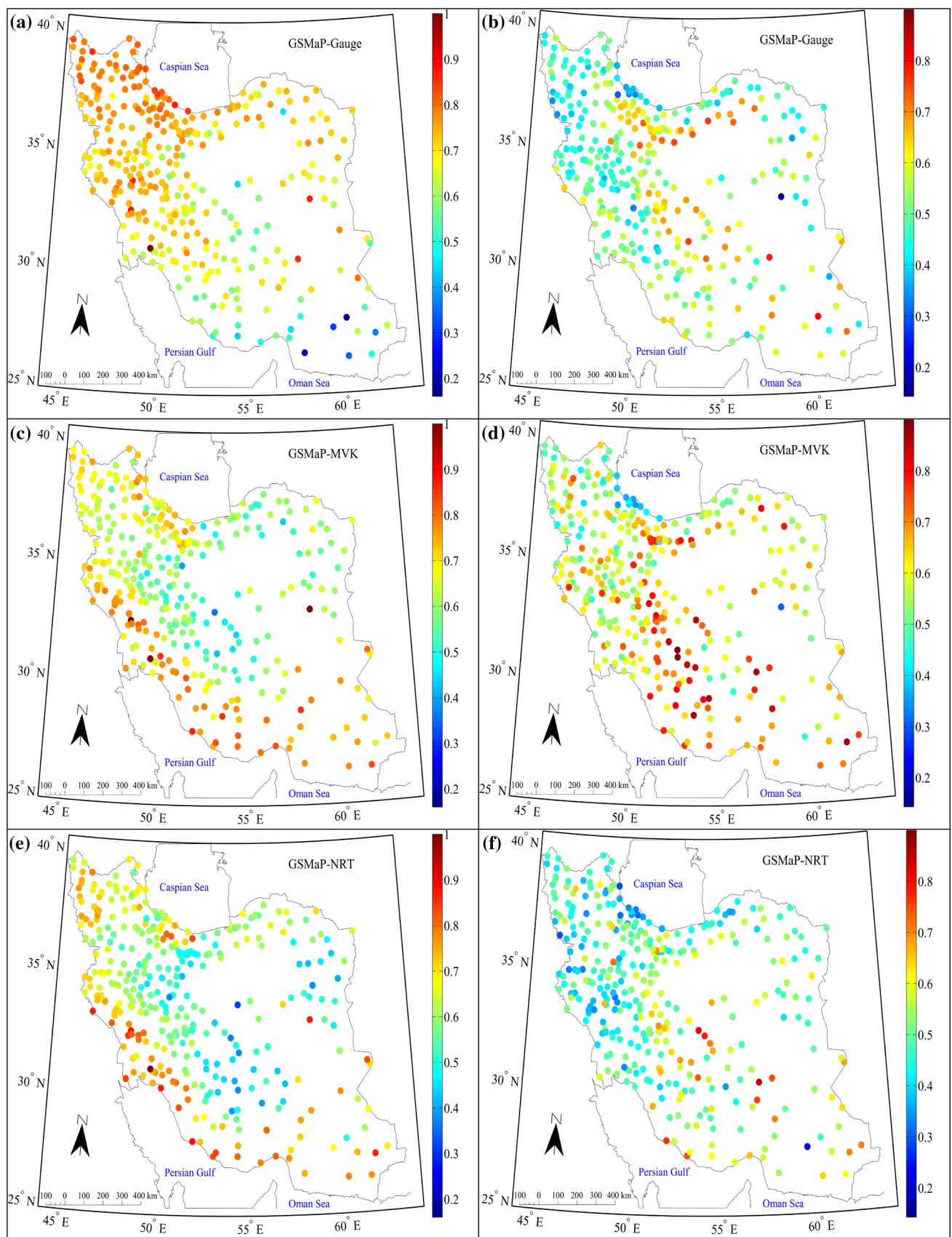


**Fig. 7** Spatial distributions of POD and FAR for GSMAp-Gauge (top panel), GSMAp-MVK (middle panel), and GSMAp-NRT (bottom panel) versus observation

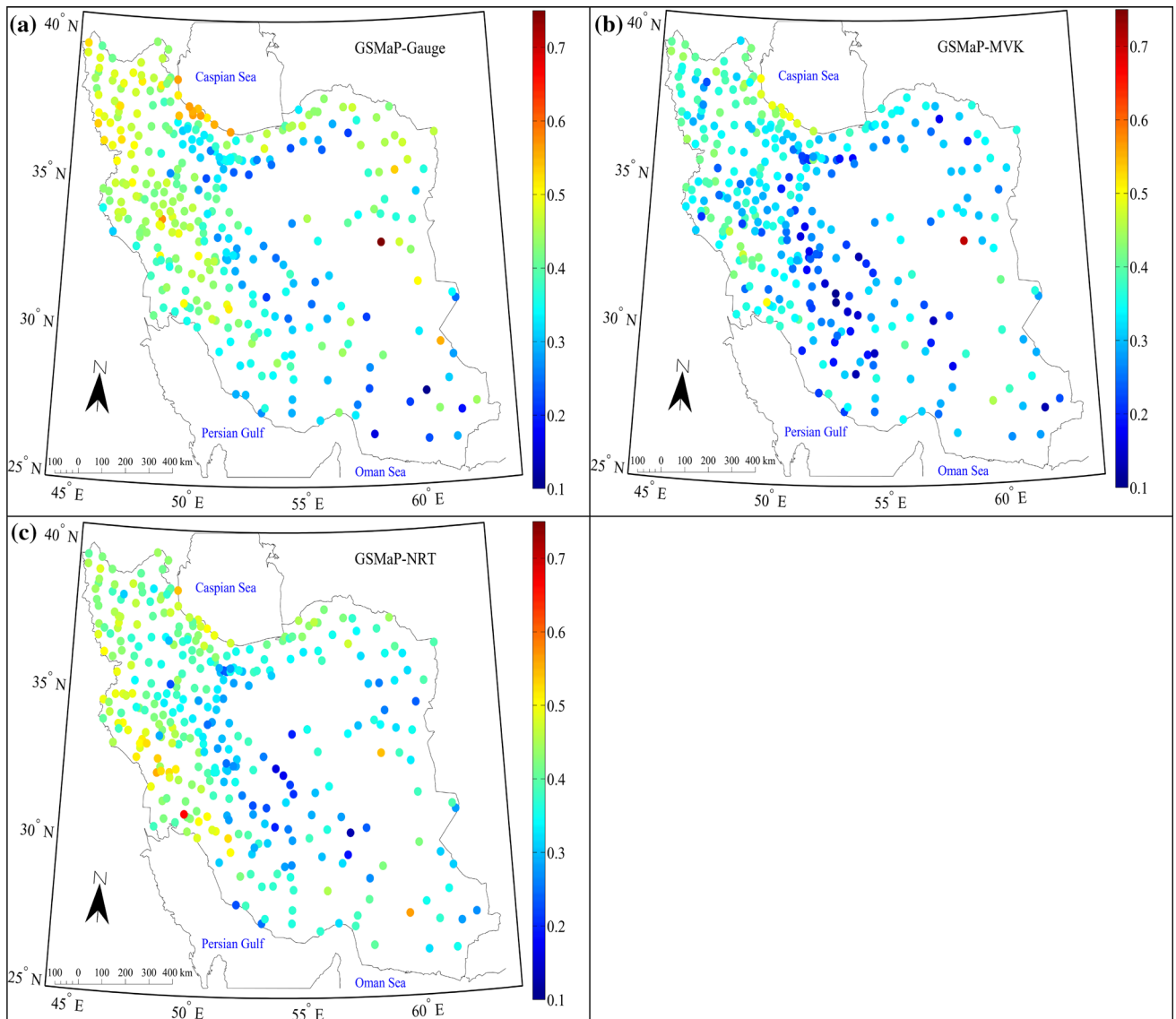


**Fig. 8** Same as Fig. 7, but for CSI

Overall, the results revealed that GMSaP-Gauge offers the option to be used in hydro climatological applications, and has the potential to promote them. However, a region-specific bias correction is required before it can be used in

climatological and hydrological applications, which is worthy of attention on the part of product developers in further refinement of the retrieval algorithms to better track the sources of error and improve the accuracy of the product.

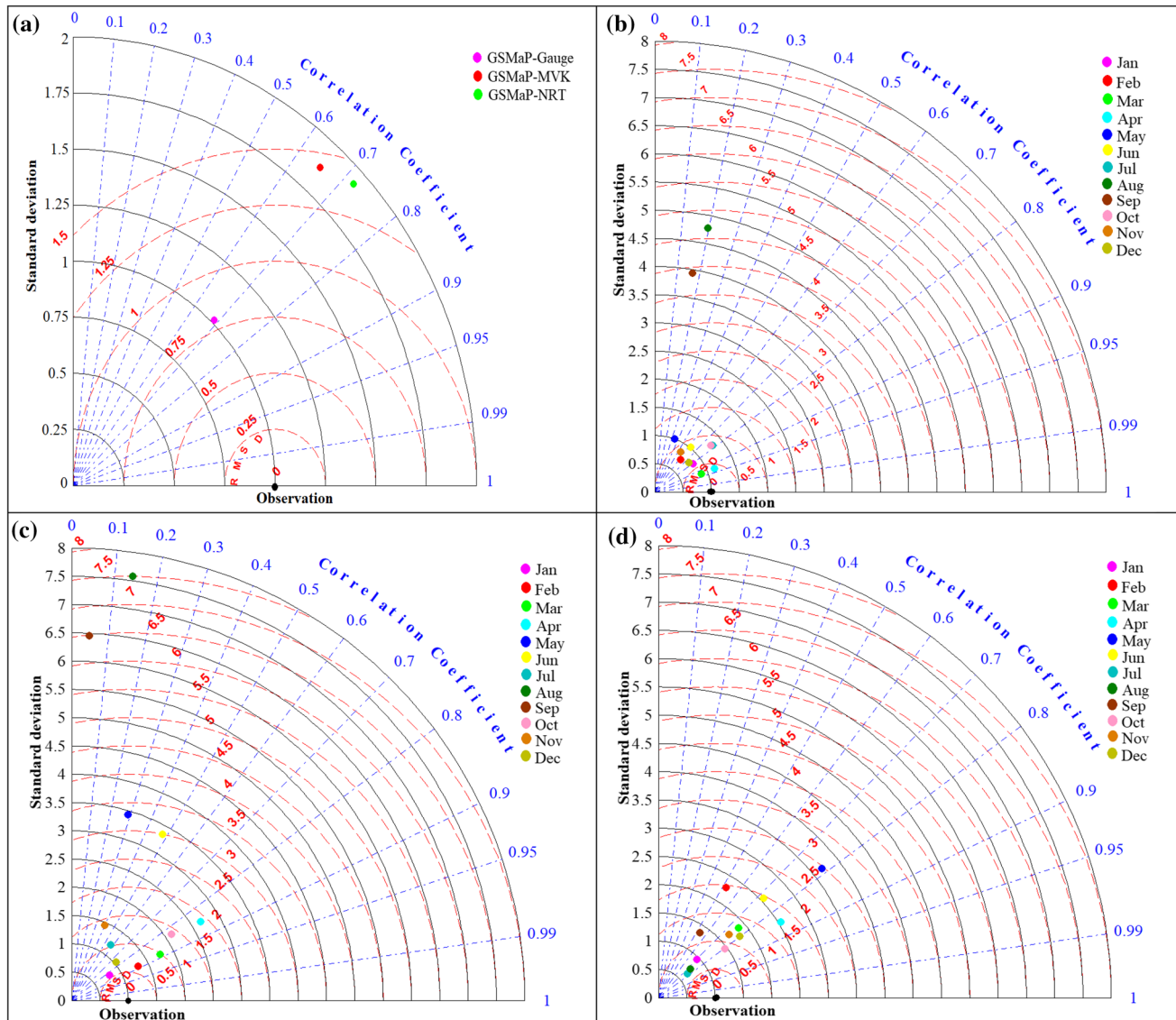


**Fig. 9** Taylor diagrams showing the comparison of daily (a) and monthly precipitation for the GSMAp products (GSMAp-Gauge (b), GSMAp-MVK (c), and GSMAp-NRT (d)) with respect to the gauge-observation data

**Acknowledgements** The authors would like to express their gratitude to the Japan Aerospace Exploration Agency (JAXA) for providing GSMAp precipitation data and to the Iranian Meteorological Organization (IRIMO) for providing gauge-observation data.

## References

- Beck HE, Vergopolan N, Pan M, Levizzani V et al (2017) Global-scale evaluation of 22 precipitation datasets using gauge observations and hydrological modeling. *Hydrol Earth Syst Sci* 21:6201–6217. <https://doi.org/10.5194/hess-21-6201-2017>
- Behrangi A, Andreadis K, Fisher JB, Turk FJ, Granger S, Painter T, Das N (2014) Satellite-based precipitation estimation and its application for stream flow prediction over mountainous western U.S. basins. *J Appl Meteorol Climatol* 53(12):2823–2842. <https://doi.org/10.1175/jamc-d-14-0056.1>
- Chen S, Hong Y, Cao Q, Gourley JJ, Kirtstetter PE, Yong B, Tian Y, Zhang Z, Shen Y, Hu J, Hardy J (2013) Similarity and difference of the two successive V6 and V7 TRMM multisatellite precipitation analysis performance over China. *JGR Atmos* 118(23):1–10
- Chen S, Behrangi A, Tian Y et al (2016) Precipitation spectra analysis over China with high-resolution measurements from optimally-merged satellite/gauge observations-part II: diurnal variability analysis. *IEEE J Sel Topics Appl Earth Observ Remote Sens* 9:2979–2988
- Cifelli R, Chandrasekar V, Lim S, Kennedy PC, Wang Y, Rutledge SA (2011) A new dual-polarization radar rainfall algorithm: application in Colorado precipitation events. *J Atmos Ocean Technol* 28:352–364
- Darand M, Mirzaei N (2020) The relationships between precipitation, rain days, and relative vorticity of the mid-troposphere 500 hPa over Iran. *Weather* 74:23–31

- Darand M, Amanollahi J, Zandkarimi S (2017) Evaluation of the performance of TRMM Multi-satellite Precipitation Analysis (TMPA) estimation over Iran. *Atmos Res* 190:121–127. <https://doi.org/10.1016/j.atmosres.2017.02.011>
- Deng P, Mingyue Zh, Guo H et al (2018) Error analysis and correction of the daily GSMAp products over Hanjiang River Basin of China. *Atmos Res* 214:121–134. <https://doi.org/10.1016/j.atmosres.2018.07.022>
- Dinku T, Ruiz F, Connor SJ, Ceccato P (2010) Validation and inter-comparison of satellite rainfall estimates over Colombia. *J Appl Meteorol Climatol* 49:1004–1014. <https://doi.org/10.1175/2009JAMC2260.1>
- Fatkhuroyan F, Wati T, Sukmana A, Kurniawan R (2018) Validation of Satellite Daily Rainfall estimates over Indonesia. *Forum Geografi* 31(2):170–180
- Fu Q, Ruan R, Liu Y (2011) Accuracy assessment of Global Satellite Mapping of Precipitation (GSMAp) product over Poyang Lake basin, China. *Procedia Environ Sci* 10:2265–2271
- Gebregiorgis AS, Kirstetter PE, Hong YE, Carr NJ, Gourley JJ, Petersen W, Zheng Y (2017) Understanding overland multisensor satellite precipitation error in TMPA-RT products. *J Hydrometeorol* 18:285–306. <https://doi.org/10.1175/JHM-D-15-0207.1>
- Hosseini-Moghari SM, Tang Q (2020) Validation of GPM IMERG V05 and V06 Precipitation Products over Iran. *J Hydrometeorol* 21:1011–1037. <https://doi.org/10.1175/JHM-D-19-0269.1>
- Hur J, Raghavan SV, Nguyen NS, Liong SY (2016) Evaluation of high-resolution satellite rainfall data over Singapore. *Procedia Eng* 154:158–167
- Khodadoust Siuki S, Saghafian B, Moazami S (2017) Comprehensive evaluation of 3-hourly TRMM and half-hourly GPM-IMERG satellite precipitation products. *Int J Remote Sens* 38:558–571
- Kidd C, Huffman G (2011) Global precipitation measurement. *Meteorol Appl* 18:334–353
- Kubota T, Shige S, Hashizume H et al (2007) Global precipitation map using satelliteborne microwave radiometers by the GSMAp project: production and validation. *IEEE Trans Geosci Remote Sens* 45(7):2259–2275
- Kummerow C, Barnes W, Kozu T, Shiue J, Simpson J (1998) The Tropical Rainfall Measuring Mission (TRMM) sensor package. *J Atmos Oceanic Technol* 15:809–817
- Ning S, Wang J, Jin J et al (2016) Assessment of the latest GPM-Era high-resolution satellite precipitation products by comparison with observation gauge data over the Chinese Mainland. *Water* 8(11):481
- Okamoto KI, Ushio T, Iguchi T et al (2005) The global satellite mapping of precipitation (GSMAp) project//Geoscience and Remote Sensing Symposium, 2005. In: IGARSS 05. Proceedings. 2005 IEEE International. IEEE, pp 3414–3416
- Peng B, Shi J, Ni-Meister W et al (2014) Evaluation of TRMM Multisatellite Precipitation Analysis (TMPA) products and their potential hydrological application at an Arid and Semi-arid Basin in China. *IEEE J Sel Top Appl Earth Observ Remote Sens* 7(9):3915–3930
- Petersen WA, Christian HJ, Rutledge SA (2005) TRMM observations of the global relationship between ice water content and lightning. *Geophys Res Lett* 32:2471–2494
- Prakash S, Mitra AK, Rajagopal E, Pai D (2016) Assessment of TRMM-based TMPA-3B42 and GSMAp precipitation products over India for the peak southwest monsoon season. *Int J Climatol* 36:1614–1631
- Salles L, Satge F, Roig H, Almeida T, Olivetti D, Ferreira W (2019) Seasonal effect on spatial and temporal consistency of the new GPM-based IMERG-v5 and GSMAp-v7 satellite precipitation estimates in Brazil's Central Plateau Region. *Water* 11:668. <https://doi.org/10.3390/w11040668>
- Sperber KR, Annamalai H, Kang IS, Kitoh A, Moise A, Turner A, Wang B, Zhou T (2013) The Asian summer monsoon: an inter-comparison of CMIP5 vs. CMIP3 simulations of the late 20th century. *Clim Dyn* 41:2711–2744. <https://doi.org/10.1007/s00338-012-1607-6>
- Su Z, Fernández-Prieto D, Timmermans J et al (2014) First results of the earth observation Water Cycle Multi-Mission Observation Strategy (WACMOS). *Int J Appl Earth Obs Geoinf* 30(3):251–252
- Sugiarto N, Ogawara K, Tanaka T et al (2017) Application of GSMAp product and rain gauge data for monitoring rainfall condition of flood events in Indonesia. *Int J Environ Geosci* 1:36–47
- Sun R, Yuan H, Liu X, Jiang X (2016) Evaluation of the latest satellite-gauge precipitation products and their hydrologic applications over the Huahe River basin. *J Hydrol* 536:302–319
- Taylor KE (2001) Summarizing multiple aspects of model performance in a single diagram. *J Geophys Res* 106(D7):7183–7192
- Tian YD, Peterslidard CD, Adler RF et al (2010) Evaluation of GSMAp precipitation estimates over the contiguous United States. *J Hydrometeorol* 11(2):566–574
- Trinh-Tuan L, Matsumoto J, Ngo-Duc T, Nodzu MI, Inoue T (2019) Evaluation of satellite precipitation products over central Vietnam. *Prog Earth Planet Sci* 6:54. <https://doi.org/10.1186/s40645-019-0297-7>
- Ushio T, Sasahige K, Kubota T et al (2009) Kalman filter approach to the Global Satellite Mapping of Precipitation (GSMAp) from combined passive microwave and infrared radiometric data. *J Meteor Soc Japan* 87A:137–151
- Vergara H, Hong Y, Gourley JJ, Anagnostou EN, Maggioni V, Stamopoulos D, Kirstetter PE (2014) Effects of resolution of satellite-based rainfall estimates on hydrologic modeling skill at different scales. *J Hydrometeorol* 15:593–613. <https://doi.org/10.1175/JHM-D-12-0113.1>
- Wang H, Yong B (2020) Quasi-global evaluation of IMERG and GSMAp precipitation products over land using gauge observations. *Water* 12:243. <https://doi.org/10.3390/w12010243>
- Xie PP, Yatagai A, Chen MY, Hayasaka T, Fukushima Y, Liu CM, Yang S (2007) A gauge-based analysis of daily precipitation over East Asia. *J Hydrometeorol* 8:607–626
- Zhao H, Yang S, You S, Huang Y, Wang Q, Zhou Q (2017) Comprehensive evaluation of two successive V3 and V4 IMERG final run precipitation products over Mainland China. *Remote Sens* 10:34
- Zhao H, Yang B, Yang S, Huang Y, Dong G, Bai J, Wang Z (2018) Systematical estimation of GPM-based global satellite mapping of precipitation products over China. *Atmos Res* 201:206–217

**Publisher's Note** Springer Nature remains neutral with regard to jurisdictional claims in published maps and institutional affiliations.